CDF/ANAL/EXOTIC/CDFR/8363
Version 1.0
March 15, 2007

Search for $ZH \rightarrow l^+l^-b\bar{b}$ in 1 fb^{-1} of CDF Run 2 Data

Jonathon Efron, Ben Kilminster, Richard Hughes, Brandon Parks, Brian Winer
The Ohio State University
Beate Heinemann, Andrew Mehta
University of Liverpool

Abstract

We search for the Higgs Boson in 1 fb^{-1} from the process $ZH \rightarrow l^+l^-b\bar{b}$ in both ee and $\mu\mu$ channels. These channels have a small background of mostly real $Z+jets$ events due to the requirement of two leptons and a Z mass constraint. We loosen the tight and loose electron and muon cuts from standard high P_T (top) analyses to improve statistics. We correct the two candidate Higgs jets with an Artificial Neural Network which assigns $\not\!\!E'_{\rm T}$ to the jets according to their $\not\!\!E_{\rm T}$ projections and relative ϕ. To maintain signal efficiency and improve signal discrimination, we employ an additional neural network trained to discriminate event kinematics of ZH compared to the main $Z + jets$ background and the kinematically different $t\bar{t}$ background. This analysis improves over our previous analysis on the same dataset by a factor of 2 improvement in luminosity.

1 Introduction

This note updates the search for $ZH \rightarrow l^+l^-b\bar{b}$ described in CDF 8363 [1]. The new analysis uses the same 1 fb$^-$1 dataset as before, but makes improvements in the jet energies using a dijet energy correction function, and also by splitting the events into single and double-tagged events. A new kinematic Neural Network, using a different set of variables, is optimized to take advantage of the jet energy improvements. In addition, we have made improvements in our mistag estimations as well as their systematic shape uncertainty which is now included in the fitting procedure.

We first define selection criteria for tight and loose electrons and muons, as well as scale factors and efficiencies. We include acceptance tables for processes contributing to our signal region, comparing events between data and our expected model of the data. We introduce a two-dimensional Neural Network trained to separate ZH, $Z + jets$ and $t\bar{t}$ using nine event kinematic variables. We demonstrate its performance in pretagged data. We introduce a fit method which allows us to fit for ZH signal, and evaluate an a priori expected limit. The data is shown compared to our background model for input kinematics and the output discriminant. We cover a full range of shape and normalization systematics. Cross-checks on the resulting fit method are done.

2 Data and Monte Carlo Samples

The data sample includes all the data up to the February 2006 shutdown. They were taken with the inclusive high p_T lepton triggers: `ELECTRON_CENTRAL_18`, `CMUP_18` and `CMX_18` which require at least one central electron with $E_T > 18$ GeV, or a CMUP or CMX muon with $p_T > 18$ GeV. The goodrun list version 13 is used [2]:

- for electrons we require electrons, silicon, COT and calorimeter to be good and obtain an integrated luminosity of 1.019 fb^{-1}
- for muons we require CMUP, CMX, silicon, COT and calorimeter to be good and obtain an integrated luminosity of 0.973 fb^{-1}. The CMX is not used for runs < 150145.

The following Monte Carlo samples are used for the Standard Model background:

- Alpgen $Z + b\bar{b}$ with $Z \to ee$ is used to model this background. The sample used is `ztop0b`.

- Alpgen $Z + c\bar{c}$ with $Z \to ee$ is used to model this background. The sample used is `ztop2b`.

- Alpgen $Z + 2p$ is used to compare data and MC before requiring a b-tag to verify in a high statistics sample the modelling of the simulation. The cross section is taken to be 25 pb and the sample used is called `atop4z`.

- $t\bar{t}$ is modelled using Pythia, and the datasets used are `ttopkl` and `ttopel`. We assume the NNLO cross section calculation of $\sigma_{t\bar{t}} = 7.3$ pb at $m_t = 175$ GeV.

- WZ and ZZ are modelled using Pythia. The samples are `ztopcz` for ZZ and `wtop1z` for WZ. The cross sections are taken to be 1.39 pb for ZZ and 3.65 pb for WZ. These samples are filtered for two leptons. In ZZ, 6.7% of events pass our lepton filter, 6.35% in ZW.

- WW+2 jets is modelled using Alpgen but was found to be negligible.

- Z+jets with $Z \to \tau\tau$ backgrounds are estimated using the Pythia sample `ztopdi`. It is found to be negligible.

- As an alternative model for Z+ jets production we use Pythia. The differences between Pythia and Alpgen are taken as systematic uncertainty. The Pythia samples used are `ztopei`, `ztopbi`, `ztop0i` and `ztop2i`. These samples are inclusive Pythia production, and are also used to understand the overall yield of Z bosons.

All of these samples were made using 5.3.3 simulation and reconstruction. For the signal Pythia was used to generate ZH production. We have made samples at 6 different mass values: 110, 115, 120, 130, 140, and 150 GeV. In this note we focus on documenting the result assuming a mass of 120 GeV. A measurement of the 95all masses listed.

+

Selection
One high E_T -CEM, -CMUP, or -CMX triggered lepton
A second high E_T lepton of same type
ΔZ_0 of leptons < 4 cm
Opposite Sign muons or central-central electrons
Z mass window 76 GeV - 106 GeV
2 or more Cone 0.4 jets L5 $E_T > 15$ GeV, $\|\eta\| < 2$
1 or more jets with L5 $E_T > 25$ GeV
2 or more loose SECVTX tags
If not found 1 or more tight SECVTX tags

Table 1: Summary of event selection. See lepton selection tables.

3 Event Selection

An overview over the event selection criteria is given in Table 1. We require two electrons or muons with an invariant mass near the Z boson mass. and 2 or morejets. We then split our signal into two regions. We first search for and event with at least two tags as determined by the the loose SECVTX algorithem. If an event does not pass this cut, we search one tagged jet as determined by the tight SECVTX algorithem.

The lepton selection we use is looser than the "standard" selection since we are trying to gain as much acceptance as possible. The non-Z backgrounds are very small and maximising the acceptance is one of the most critical issues for the Higgs search. The lepton selection cuts are given in Tables 2 and 3 for electrons and in Tables 4 and 5 for muons.

The main differences w.r.t. the default selections are

- electrons
  - usage of tower 9 for both loose and tight electrons
  - relax the CES strip χ^2 cut to 25 for tight electron
- muons
  - relax the tracking requirements to just require at least one COT hit. That increases the acceptance at high η for loose muons.

Tight Electron Selection
$E_T > 18$ GeV *
$P_T > 9$ GeV *
Had/Em $< 0.055 + 0.00045 \cdot$E
$E/P < 2.5 + 0.015 \cdot E_T$
$\lvert Z_{vertex} \rvert < 60$ cm
CES Fiducial = 1 (or 2)*
Isolation $\cdot E_{TRAW}/E_{TCORR} < 0.1$
$L_{shr} < 0.2$
-3.0 $<$ Q $\cdot \lvert \Delta X < \rvert$ 1.5
$\chi^2_{strip} < 25.0$ *
$\lvert Z_{electron} - Z_{vertex} \rvert < 3$ cm
2 stereo and 2 axial * superlayer segments

Table 2: At least one electron in e-e events must satisfy these requirements. * indicates cuts which have been loosened compared to standard top selection.

Loose Electron Selection
$E_T > 19$ GeV * Central or $E_T > 10$ GeV * Plug
Had/Em $< 0.055 + 0.00045 \cdot$E
Isolation $\cdot E_{TRAW}/E_{TCORR} < 0.1$
$P_T > 5$ GeV (for Central region)
$\lvert Z_{vertex} \rvert < 60$ cm
Is Fiducial

Table 3: The second electrons in e-e events is subject to looser requirements. Note that the second electron may be a plug electron. * indicates cuts which have been loosened compared to standard top selection. There are also cuts which are not considered.

Tight Muon Selection
$P_T > 20$ GeV
Had Energy < 6 GeV
Em Energy < 2 GeV
CMX $\rho > 140$ cm
>= 3 axial and >=3 stereo segments
Isolation < 0.1
$\|\Delta X\|_{CMU} < 3.0$ cm
$\|\Delta X\|_{CMP} < 5.0$ cm
$\|\Delta X\|_{CMX} < 6.0$ cm
Impact parameter $d_0 < 0.2$ w/Silicon hits (0.02 w/out)

Table 4: The tight muon is currently the same as the Top group's tight selection for CMX and CMUP.

Loose Muon Selection
$P_T > 18$ GeV *
Had Energy < 6 GeV
Em Energy < 2 GeV
CMX $\rho > 140$ cm
Isolation < 0.1
Impact parameter $d_0 < 0.2$ w/Silicon hits (0.02 w/out)
>= 1 COT hits
No stub requirements *

Table 5: The loose muon selection criteria based on CMIO muons.

To account for any differences in the efficiencies of these selections we use the scale factors provided by the JointPhysics group [3]. This includes scale factors for the electron and muon identification, the b-tagging efficiency, the trigger efficiencies and the z-vertex requirement. We believe we can use these scale factors despite our looser lepton ID requirements. The scale factors for electrons are very close to 1 for any selection: this has been demonstrated in many analyses. For muons the loose ID scale factor is also close to unity.

Table 6 shows the efficiencies of the cuts for the various MC samples for electrons and muons separately at different stages of the selection.

Tables 8 and 7shows expected events for various Higgs masses.

Acceptance of $ZH \to l^+l^-bb$ events	e^+e^-	$\mu^+\mu^-$	Total
Tight Lepton found	21.3%	15.2%	37.0%
Second Lepton found	12.6%	10.6%	23.4%
Z cut	11.4%	9.75%	21.2%
$\geq$2 Jets	9.36%	8.05%	17.1%
+ B-tagged	5.41%	4.73%	10.1%
2 loose B tags	1.88%	1.68%	3.55%
1 tight B-tagged	2.83%	3.31%	7.14%
With branching ratios for $Z \to l^+l^-$ and $H \to bb$			
A_{ZH}	0.368%	0.317%	0.686%

Table 6: Acceptance of $ZH \to l^+l^-b\bar{b}$ when $M_H = 120GeV/c^2$ and Z is forced to decay to charged leptons (including τs). The last line shows the acceptance of all ZH events assuming a branching ratio of $Z \to l^+l^-$=10.1% and a branching ratio of Higgs with $m_H = 120$ GeV/c^2 is of 67%

Higgs Mass	σ_{ZH} (pb)	$H \to bb$	e^+e^- events	$\mu^+\mu^-events$	Total events
$M_H = 100$ GeV/c^2	0.17	0.81	0.185	0.214	0.399
$M_H = 110$ GeV/c^2	0.12	0.77	0.144	0.165	0.309
$M_H = 115$ GeV/c^2	0.11	0.73	0.125	0.142	0.267
$M_H = 120$ GeV/c^2	0.09	0.68	0.101	0.117	0.218
$M_H = 130$ GeV/c^2	0.07	0.53	0.066	0.078	0.144
$M_H = 140$ GeV/c^2	0.05	0.34	0.037	0.043	0.080
$M_H = 150$ GeV/c^2	0.04	0.18	0.015	0.016	0.031

Table 7: Expected $ZH \to l^+l^-b\bar{b}$ events after double tag selections for range of Higgs masses. Cross-section and branching ratio taken from John Conways' SM Higgs tables.

Higgs Mass	σ_{ZH} (pb)	$H \to b\bar{b}$	e^+e^- events	$\mu^+\mu^- events$	Total events
$M_H = 100$ GeV/c^2	0.17	0.81	0.386	0.454	0.840
$M_H = 110$ GeV/c^2	0.12	0.77	0.292	0.334	0.626
$M_H = 115$ GeV/c^2	0.11	0.73	0.252	0.287	0.539
$M_H = 120$ GeV/c^2	0.09	0.68	0.201	0.233	0.434
$M_H = 130$ GeV/c^2	0.07	0.53	0.125	0.146	0.271
$M_H = 140$ GeV/c^2	0.05	0.34	0.066	0.079	0.145
$M_H = 150$ GeV/c^2	0.04	0.18	0.026	0.030	0.056

Table 8: Expected $ZH \to l^+l^-b\bar{b}$ events after single tag (not including double tag) selection for range of Higgs masses. Cross-section and branching ratio taken from John Conways' SM Higgs tables.

4 Neural Network dijet energy corrections

Since the only sources for $\not\!\!E_{\rm T}$ in $ZH \to l^+l^-b\bar{b}$ events are jet energy mismeasurement, we employ a correction function to reassign missing energy to the jets. This procedure is described in CDF 8124 [8]. This correction function is derived from ZH Monte Carlo events, and is only applicable to this final state. It is essentially a parton-jet transfer function which makes use of the correlations between the jet energies and directions and that of the $\not\!\!E_{\rm T}$. These improved jet energies are used to calculate the input kinematics for our signal to background discriminant, including most importantly, the dijet mass which is a direct measure of the Higgs mass.

The function takes as inputs the $\not\!\!E_{\rm T}$, $\not\!\!E_{\rm T}\phi$, first and second jet transverse energies of JETCLU cone 0.4 jets corrected to Level 5, their ηs and ϕs, and the transverse projections of the jets onto the $\not\!\!E_{\rm T}$ direction. The function produces two outputs which are scale factors to correct the first and second jet energies. The directions of the jets are not changed.

A Neural Network produces this function by training on the inputs mentioned above in ZH MC and attempting to reproduce the true parton energies available from the MC hepg banks. Training is done with a wide range of Higgs masses from 60 GeV/c^2 to 180 GeV/c^2 in steps of 10 Gev/c^2. The wide range of masses is used in order to prevent the Neural Network from overtraining on a particular mass which would cause the function to produce corrections biased towards that mass. To ensure that there is no bias, we do a linearity test of the NN function on independent MC events.

We also test this function on background events to make sure that background distribu-

tions are not sculpted such that an increased amount of background were contained within a region around the Higgs dijet mass peak. To do this, we construct 2 σ windows around the ZH dijet mass peak before and after the jet correction functions are applied, and we verify that the signal to background discrimination is improved in the latter catgegory. The backgrounds considered for this study are Z+jets backgrounds which have the largest contribution to the background estimation, and dilepton $t\bar{t}$ which has real $\not\!\!E_{\rm T}$ due to the W decays. $S/\sqrt{B}$ is found to improve in the case of both backgrounds, and the shape of the backgrounds is not distorted.

The NN dijet correction function is applied in the same way to data and MC. We validate the function by comparing the event kinematics, such as jet E_Ts, $\not\!\!E_{\rm T}$, H_T, of our background models of pretagged and tagged data before and after the function is applied. The plots showing the kinematics after the corrections are applied are in section5. Plots showing kinematics before the jet corrections are applied can be seen in CDF note 8363.

5 Comparison of Data to Standard Model Background

The background consists of three components:

1. Background with two genuine leptons and a genuine b- or c-jet are estimated using the MC samples described in Section 2.

2. Backgrounds with fake electrons are estimated using lepton fake rates [4]. These fake rates are determined from jet data. To remove real electrons, the "trigger jet" which is ussually the electron is removed. $\not\!\!E_{\rm T} < 15$ GeV/c^2 removes W events. The Z contribution is tiny. Rates are consistent across Jet-20, Jet-50, Jet-70, and Jet-100 samples, indicating that there is no residual Z background: it would be the largest in the Jet-100 sample but we do not see any contamination compared to the other samples. A 50% uncertainty is assigned to these lepton fake rates. For muons events where both muons have the same charge are taken to estimated this contribution. This procedure was also used for the $Z + b$ cross section measurement [5].

3. Backgrounds with a mistagged light jet are estimated using the mistag matrix [6].

   The mistag matrix is applied to the pretagged data sample and is used to estimate the number of negative SECVTX tags in the sample. For the double tagged sample, we apply the mistag matrix over pairs of two taggable jets in the pretag sample to find the predicted number of double loose negative tag events.

   To find how many events have a positive tagged light flavor jet, we apply the appropiate asymetry [7] on a jet by jet basis. We then subtract the shape that our heavy flavor backgrounds contribute to this number. [10]

The number of expected and observed events is given at various selection stages in Tables 9 for muons and 10 for electrons.

For the muons the data agree with the expectation to better than 1% for the inclusive Z selection. After requiring two jets the data are about 14% higher than the MC. We observe 5 events with two b-taggs, and 46 more with a single b-tag. This compares to 4.61 and 40.4 events predicted respectively.

For the electrons we observe about 6% more events in data than predicted by MC. We have not yet evaluated the systematic uncertainty on the prediction but it will likely be about 4% and thus nearly cover this difference. We will further investigate whether there is any problem. After requiring 2 jets we find the data yield to be 14% higher than in the simulation. We observe 6 events with two b-taggs, and 54 more with a single b-tag. This compares to 6.90 and 61.7 events predicted respectively.

The number of negative tags is also in good agreement with the prediction for both electrons and muons.

The largest background after the full selection is $Z+$ jets production followed by $t\bar{t}$ production. Combining both electrons and muons we anticipate 0.64 ZH events assuming the Standard Model cross section value.

Sample	2 Leptons	Z Selected	$\geq$1 Jet	$\geq$ 2 Jets	2 loose	1 tight (!=2loose)
ZH_{120GeV/c^2}	0.62	0.58	0.56	0.49	0.10	0.19
$t\bar{t}$	29.3	7.0	6.9	6.00	1.32 ± 0.27	2.33 ± 0.48
ZW	29.8	26.5	17.7	12.4	0.017 ± 0.003	0.51 ± 0.10
ZZ	43.8	38.6	22.9	17.1	0.58 ± 0.11	1.82 ± 0.36
$WW2p$	24.4	5.89	3.30	1.49	0.008 ± 0.002	0.020 ± 0.004
$Z \rightarrow \tau\tau$	320.1	11.3	1.04	0.42	0.00	0.00
fakes	1693	343	53	20	0.1 ± 0.1	1 ± 1
$Z^0 \rightarrow \mu^+\mu^-$	52500	45790	4218	1028	3.25 ± 1.01	35.1 ± 7.0
(b events)	648	576	144	49.8	$2.46 \pm .99$	14.5 ± 5.8
(c events)				106	0.43 ± 0.17	8.2 ± 3.3
(mistags)	Predicted mistags from data:				$0.36 \pm .09$	12.4 ± 2.1
Total	54,600	46,200	4320	1090	5.06 ± 1.05	40.8 ± 7.1
Data (972 pb^{-1})	56,740	47,982	4128	1240	5	46
Negative Tags	Predicted:				0.27	11.02 ± 0.72
	Found				1	12

Table 9: Amount of expected and observed events in the muon data at various cuts in the event selection. Until better cross sections of the heavy flavor Alpgen + Herwig is attained, the Top group's pythia is used to find b and c content normalizations. Errors shown are from systematics.

6 Neural Network Inputs

To further improve signal to background discrimination after event selection, we employ an artifical Neural Network (NN) trained on a variety of kinematic variables to distinguish ZH from backgrounds. We use the OSU RootJetnet interface to the Jetnet neural network program.

We first define a set of variables we expect to have differences between ZH and the other backgrounds, the largest two being $Z + jets$ and $t\bar{t}$. We refer to the object constructed from the two leptons as the Z, although due to fake leptons, this may not be so in data. The inclusive set of variables are :

- Z mass
- $\not\!\!E_T$ projected on jet 1
- $\not\!\!E_T$ projected on jet 2
- $\not\!\!E_T$ projected on all jets

Sample	2 Leptons	Z Selected	$\geq$1 Jet	$\geq$ 2 Jets	2 loose	1 tight(!=2loose)
ZH_{120GeV/c^2}	0.83	0.76	0.73	0.63	0.13	0.25
$t\bar{t}$	36.9	9.01	8.77	7.69	$1.52 \pm .29$	2.91 ± 0.56
ZW	46.3	40.8	25.89	18.0	0.024 ± 0.005	0.72 ± 0.14
ZZ	61.4	54.0	29.7	21.5	0.76 ± 0.15	2.16 ± 0.43
$WW2p$	33.5	7.93	4.36	2.05	0.006 ± 0.001	0.040 ± 0.008
$Z \rightarrow \tau\tau$	536	26.9	2.75	0.84	0.00	0.00
fakes	1191	322.8	42.0	15.7	0.134 ± 0.067	0.89 ± 0.44
$Z^0 \rightarrow e^+e^-$	96,440	84,940	6943	1607	5.02 ± 1.52	54.1 ± 10.7
(b events)	1019	908	209	69.5	3.81 ± 1.48	20.6 ± 8.76
(c events)				161	0.58 ± 0.22	13.6 ± 5.21
(mistags)	Predicted mistags from data:				0.63 ± 0.15	19.9 ± 3.38
Total	98,340	85,400	7082	1673	7.36 ± 1.56	60.8 ± 10.7
Data (1019 $pb^{-}1$)	102,820	88242	6423	1794	6	54
Negative Tags	Predicted:				0.44 ± 0.04	17.2 ± 1.38
	Found				0	11

Table 10: Amount of expected and found events in the electron data at various cuts in the event selection. Errors are from systematics.

- Z projected on all jets
- Number of Tight Jets (Cone 0.4)
- P_T of Z
- E_T of jet 1
- E_T of jet 2
- η of Z
- η of jet 1
- η of jet 2
- Corrected $\not\!\!E_T$
- H_{T_1} : sum of $\not\!\!E_T$, all tight jet E_Ts, and lepton E_Ts
- H_{T_2} : sum of $\not\!\!E_T$, first two jet E_Ts, and lepton E_Ts
- sig Extra E_T: Sum of Z E_T and two jets

- delE_T: E_T jet 1 - E_T jet 2
- jetP_T: P_T of two jets combined
- dijet mass: Dijet invariant mass
- dRj1j2: delta R between jet 1 and jet 2
- dRj1Z: delta R between Z and jet 1
- dRj2Z: delta R between Z and jet 1
- dRjetsZ: delta R between Z and combined jet 4-vector
- dRj1Z: delta R between Z and jet 1
- dRjetsZ: delta R between Z and combined jet 4-vector
- aplanarity
- sphericity
- Total Mass : Mass of all objects in event
- Absoulute value of $\cos\theta^*$
- Mass of Z and dijet combined

To optimize the NN, we use an iterative procedure to determine the configuration which best discriminates signal and background, and which uses a minimal number of input discriminants.

This is done by first determining the best one-variable NN of all the above variables, then keeping this variable as an input, we loop over all other the variables to determine the best two-variable NN. The best N-variable network is finally selected once the N+1-variable network shows less than a percent improvement. The criteria for comparing networks is the testing error defined by how often an NN with a given configuration correctly classifies several thousand signal and background events. Once the best N-variable NN is chosen, we

then optimize the number of hidden layers, and choose a number of training epochs which prevents overtraining.

The NN output is a discriminant which varies from 0 to 1, where 0 is background and 1 is signal. We first attempted to do a 1-dimensional NN which was trained between ZH and $Z + jets$. While this was very successful at separating the two processes, we found that the shape of the NN Output for $t\bar{t}$ peaked in out signal region, reducing our signal sensitivity. Our next attempt was to do use two NNs in series, first training $t\bar{t}$ against ZH and making a cut to remove $t\bar{t}$, and next distinguishing Z+jets from ZH for which we would fit the shape of the NN distribution to obtain the measurement. We found that we could reject 82% of $t\bar{t}$ while only removing 5% of signal, as compared to a $\not\!\!E_{\rm T}$ cut which would reject the same amount of $t\bar{t}$ but remove 10% of signal. However, the 20% remaining $t\bar{t}$ peaked very strongly in the ZH signal region in the subsequent $Z + jets$ vs. ZH NN, leading to weakened signal sensitivity.

The solution is to create a 2-D NN, trained to discriminate $t\bar{t}$ vs ZH on one axis, and Z+jets vs ZH on the other axis. The optimization procedure is that described for the 1-D case above, such that the figure of merit for comparing NNs becomes the average of the testing errors for each of the 3 MCs.

Our final Neural Network configuration is 8 input variables, 17 hidden nodes, and 2 output nodes.

The optimization of the variables are shown in Figure 1, and the list in order of importance are :

- Corrected $\not\!\!E_{\rm T}$
- H_{T_2} : sum of $\not\!\!E_{\rm T}$, first two jet E_Ts, and lepton E_Ts
- dijet mass: Dijet invariant mass
- dRj1Z: delta R between Z and jet 1
- dRj1Z: delta R between Z and jet 2
- dRj1Z: delta R between jet 1 and jet 2

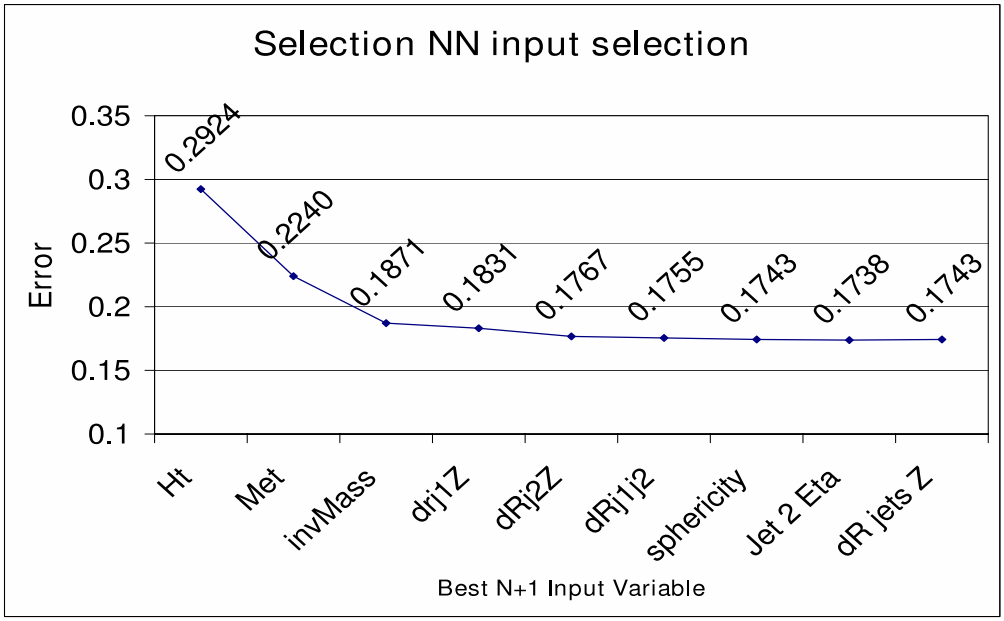

Figure 1: Optimization of NN. The top plot shows the testing error, where the x-axis is the number of variables in N in the best N-variable NN. Adding in the best 9th variable does not show improvement.

- sphericity
- Jet 2 η
- Not used: the next best variable would be the $\not\!\!E_{\rm T}$ projected on the first jet.

The Neural Net output distributions are shown for all the backgrounds in Fig. 2 and 3 for the single-tagged sample. These templates are used in all subsequent studies. It is seen that the ZH signal is primarily at $(0, 1)$, the $t\bar{t}$ background mostly at $(1, 1)$ and most other backgrounds are at $(0, 0)$ in this space.

One of the strengths of a artificial neural network is that it can exploit correlations between inputs that are not obvious. In Table 11, the correlations of the training signals and backgrounds are shown. In Table 12 and 13, the correlations of the input variables to both output dimensions are shown in the same signal and background samples.

6.1 Comparison of Data and MC in the Pretag Sample

It is crucial to test whether the input variables of the Neural Net are modelled well by the simulation. An excellent control sample to understand this modelling is the pretag sample,

Correlation	ZH	$t\bar{t}$	Z+$b\bar{b}$	Z+$c\bar{c}$	ZZ
Mass – Ht	0.236	0.285	0.427	0.421	0.365
Mass – Met	0.0105	0.0154	0.126	0.0507	0.119
Mass – Drj1j2	0.381	0.74	0.707	0.718	0.371
Mass – Drj1Z	-0.0564	-0.235	-0.14	-0.15	-0.0736
Mass – Drj2Z	-0.177	-0.237	-0.298	-0.353	-0.163
Mass – Sph	0.0868	-0.0141	0.0222	0.0348	-0.0134
Mass – Jet2Eta	-0.00735	0.01	-0.00265	-0.0222	-0.0389
Ht – Met	0.082	0.458	0.236	0.223	0.258
Ht – Drj1j2	-0.597	-0.127	-0.0988	-0.0952	-0.497
Ht – Drj1Z	0.113	-0.343	-0.0728	-0.0664	-0.053
Ht – Drj2Z	0.178	-0.0724	-0.105	-0.139	0.0601
Ht – Sph	-0.176	-0.148	-0.0571	-0.0624	-0.128
Ht – Jet2Eta	-0.00378	-0.0386	-0.0181	-0.00457	-0.0259
Met – Drj1j2	0.0757	-0.128	0.0457	-0.051	-0.032
Met – Drj1Z	-0.026	-0.16	-0.0378	-0.00493	-0.0829
Met – Drj2Z	-0.07	0.194	-0.0423	0.00167	0.0532
Met – Sph	-0.102	-0.00288	-0.0657	-0.0411	-0.0843
Met – Jet2Eta	0.00413	-0.0241	-0.00626	0.00413	0.0159
Drj1j2 – Drj1Z	-0.073	-0.155	-0.092	-0.107	0.000374
Drj1j2 – Drj2Z	-0.489	-0.265	-0.392	-0.424	-0.33
Drj1j2 – Sph	0.0923	-0.0774	0.0348	0.0873	0.0842
Drj1j2 – Jet2Eta	-0.000673	0.0141	0.00778	-0.0269	0.0137
Drj1Z – Drj2Z	-0.0839	-0.125	0.127	0.165	0.107
Drj1Z – Sph	-0.236	0.0135	-0.29	-0.331	-0.225
Drj1Z – Jet2Eta	0.000466	-0.00422	0.0322	-0.0177	-0.000403
Drj2Z – Sph	0.00832	0.0685	-0.103	-0.148	-0.0762
Drj2Z – Jet2Eta	-0.0122	-0.00566	0.00601	0.0119	-0.0299
Sph – Jet2Eta	0.121	0.243	0.0453	0.0632	0.0262

Table 11: List of correlations between input variables of the selected artificial neural network for the signal (ZH) and the various backgrounds. ZH ($M_H = 120$ GeV/c^2) is targeted during training of the $SANN^2$ to corner (1,0). Z+$b\bar{b}$ and Z+$c\bar{c}$ are targeted during training of the $SANN^2$ to corner (0,0); $t\bar{t}$ is targeted during training of the $SANN^2$ to corner (1,1). ZZ is also shown for a referance of a background that is similar to ZH.

Input Variable	ZH	$t\bar{t}$	Z+$b\bar{b}$	Z+$c\bar{c}$	ZZ
Mass	0.529	0.112	0.532	0.571	0.459
Ht	0.437	0.475	0.484	0.505	0.539
Met	-0.0195	0.603	0.167	0.149	0.18
dRj1j2	-0.0706	-0.192	0.273	0.299	-0.137
dRj1Z	-0.217	-0.347	-0.329	-0.326	-0.341
dRj2Z	-0.223	-0.0225	-0.377	-0.375	-0.314
sph	0.201	0.0634	0.188	0.173	0.142
Jet2Eta	-0.000294	0.0331	-0.0355	-0.000194	0.00531

Table 12: List of correlations between input variables and the discriminate of Z+jets and ZH. The selected artificial neural network for the signal (ZH) and the various backgrounds. ZH (M_H = 120 GeV/c^2) is targeted during training of the $SANN^2$ to corner (1,0). Z+$b\bar{b}$ and Z+$c\bar{c}$ are targeted during training of the $SANN^2$ to corner (0,0); $t\bar{t}$ is targeted during training of the $SANN^2$ to corner (1,1). ZZ is also shown for a referance of a background that is similar to ZH.

Input Variable	ZH	$t\bar{t}$	Z+$b\bar{b}$	Z+$c\bar{c}$	ZZ
Mass	0.275	0.244	0.463	0.468	0.33
Ht	0.0626	0.618	0.303	0.278	0.324
Met	0.589	0.85	0.561	0.47	0.699
dRj1j2	0.114	-0.117	0.234	0.23	0.0177
dRj1Z	-0.196	-0.322	-0.221	-0.219	-0.22
dRj2Z	-0.0184	0.083	-0.108	-0.109	0.03
sph	0.02	-0.0149	0.00215	0.0161	-0.0313
Jet2Eta	-0.00679	-0.0198	-0.00765	-0.000533	0.0197

Table 13: List of correlations between input variables and the discriminate of $t\bar{t}$ and ZH. The selected artificial neural network for the signal (ZH) and the various backgrounds. ZH (M_H = 120 GeV/c^2) is targeted during training of the $SANN^2$ to corner (1,0). Z+$b\bar{b}$ and Z+$c\bar{c}$ are targeted during training of the $SANN^2$ to corner (0,0); $t\bar{t}$ is targeted during training of the $SANN^2$ to corner (1,1). ZZ is also shown for a referance of a background that is similar to ZH.

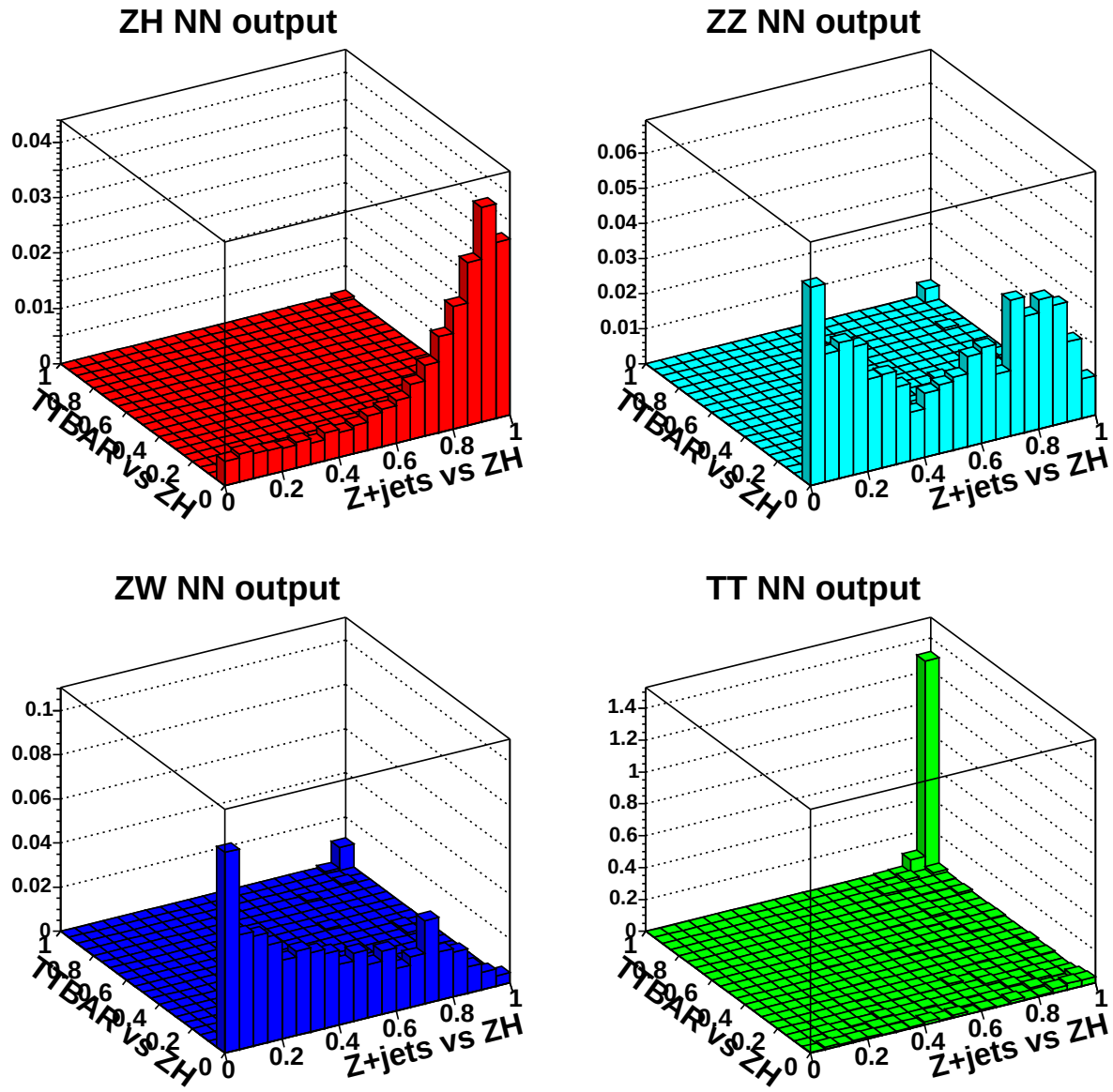

Figure 2: The NN distribution templates for ZH (red, upper left), ZZ (cyan, upper right), ZW (blue, lower left), $t\bar{t}$ (green, lower right).

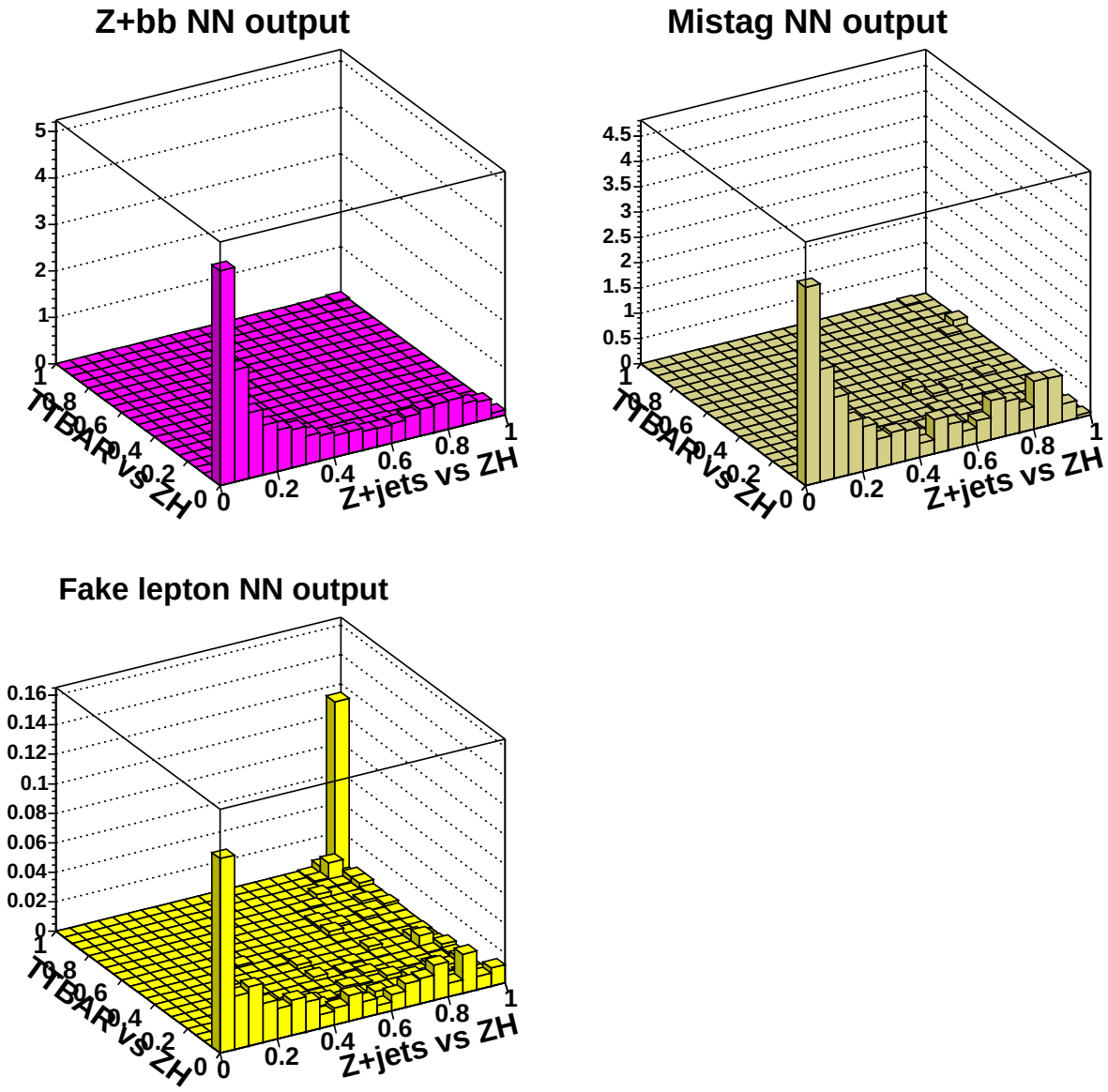

Figure 3: The NN distribution templates for $Z + bb$ (pink, upper left), fakes (yellow, lower left), mistags (drab, upper right).

i.e. the $Z + 2$ jets events before requiring a b tag.

The comparison of data to AlpGen+Herwig samples and Pythia are overlaid and is shown for electrons in in Fig. 4-5.

The data are generally well modelled by the simulation. Only at low H_T, and low jet E_T values the simulation undershoots the data. This difference is accounted for in the systematic uncertainty that we include by using Pythia instead of Alpgen. It is seen that Pythia gives generally a poorer desciption of the data, particularly at high H_T and high dijet mass. However, it agrees well at low values of H_T and jet E_T. Thus we think that taking Pythia for the systematic uncertainty is a fair assessment of the modelling of the shape of this background.

6.2 Variable Correlations in the Neural Network

Variable correlations are also important for a multivariate approach. We use the following definition for an event by event correlation between two generic variables x and y:

$$corr(x, y) = \frac{(x - \overline{x}) \cdot (y - \overline{y})}{(\Delta x \cdot \Delta y)^{1/2}}, \tag{1}$$

where $\overline{x}$ is the average and $\Delta x = \overline{(x - \overline{x})^2}$ for the distribution in the x variable.

Comparisons between a simulated model and pretagged data in the $Z+ >= 2$ jets events (electrons only) are presented in Figure 6. The model here is a combination backgrounds according to Table 10. The most important variables to the Neural Network, determined through the optimization procedure described in section 6, are H_T, $\not\!\!E_{\rm T}$, and M_{jj}. For a quantitative evaluation of the compatibility between the two shapes, the KS test has been calculated for the 3 distributions shown, with the results of 0.98 for H_T:M_{jj}, 0.76 for H_T:$\not\!\!E_{\rm T}$, and 0.40 for M_{jj}:$\not\!\!E_{\rm T}$. Although the correlations are still the subject of further study, there is reasonably good agreement for this subsample of variables.

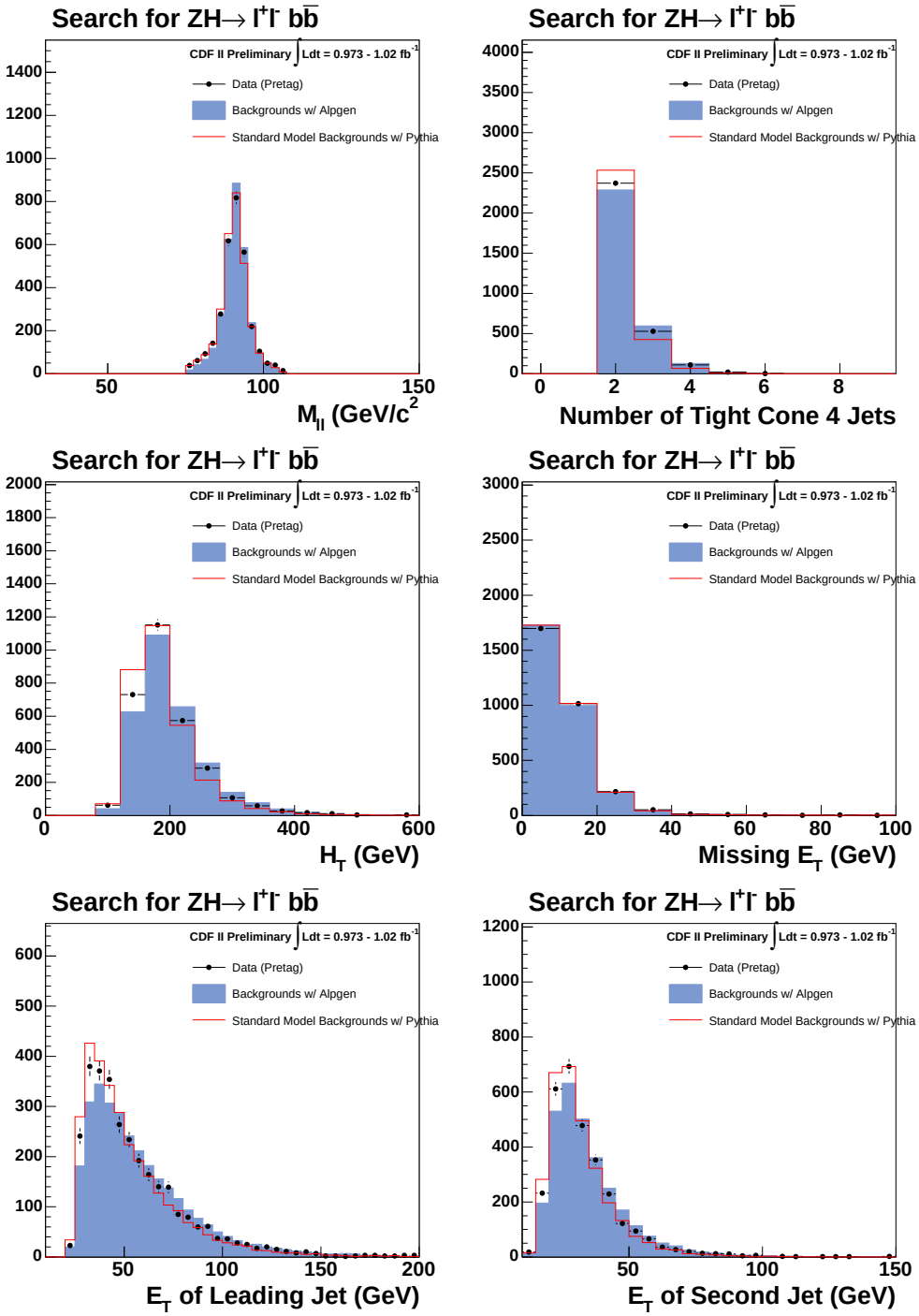

Figure 4: Pretagged data compared to Monte Carlo expectation. The MC which uses the Alpgen+Herwig montecarlo simulations are in blue, pythia is represented with the red line: invariant dilepton mass (upper left), number of jets (upper right), H_T (middle left), missing E_T (middle right), E_T of leading (lower left) and subleading (lower right) Jets.

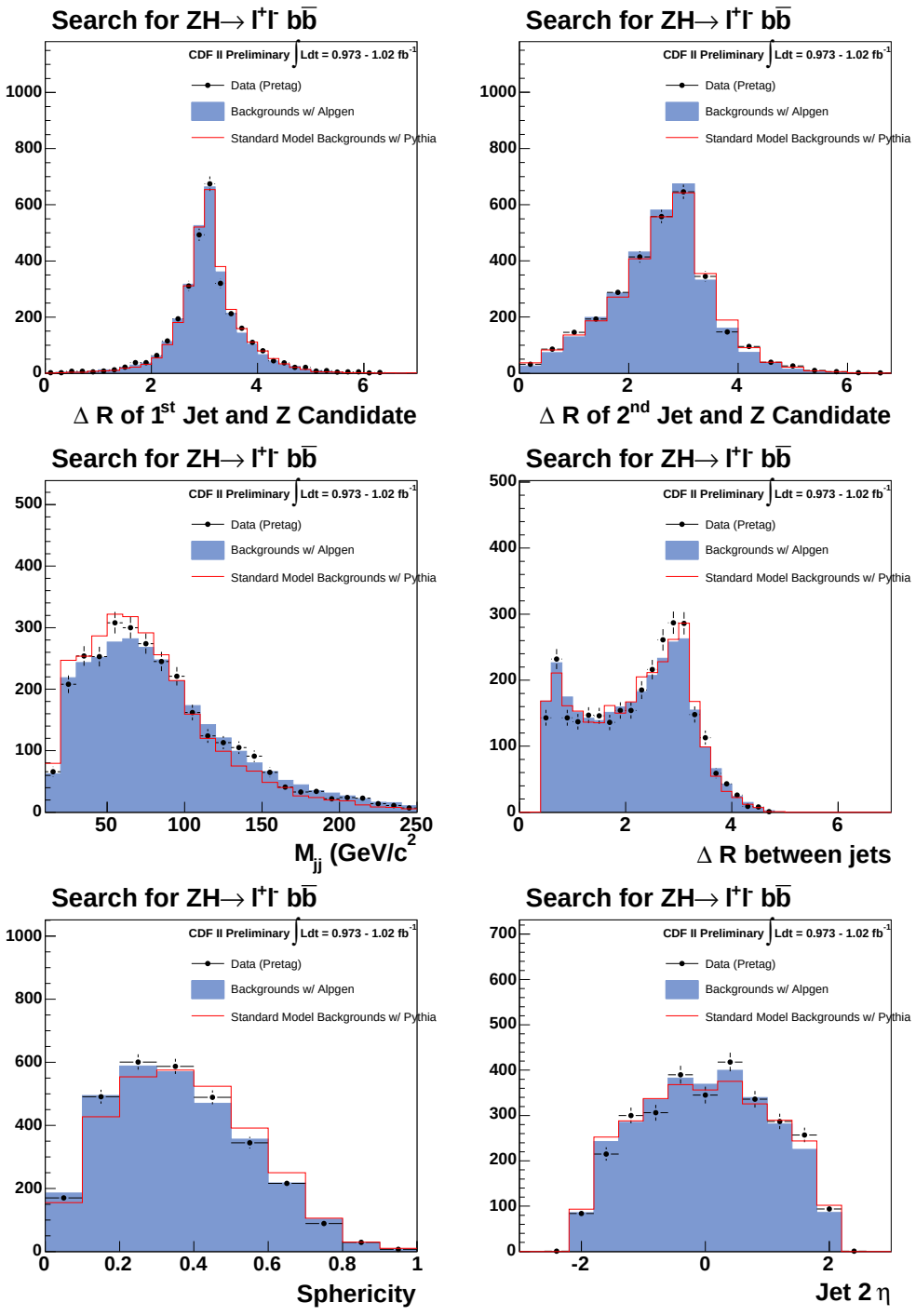

Figure 5: Pretagged data compared to Monte Carlo expectation. The MC which uses the Alpgen+Herwig montecarlo simulations are in blue, pythia is represented with the red line: ΔR of leading jet and Z (upper left), ΔR of second jet and Z (upper right), invariant mass of two leading jets (middle left), ΔR of leading and second jets (middle right), sphericity of 4 relevant objects (bottom left), η of second jet (bottom right.)

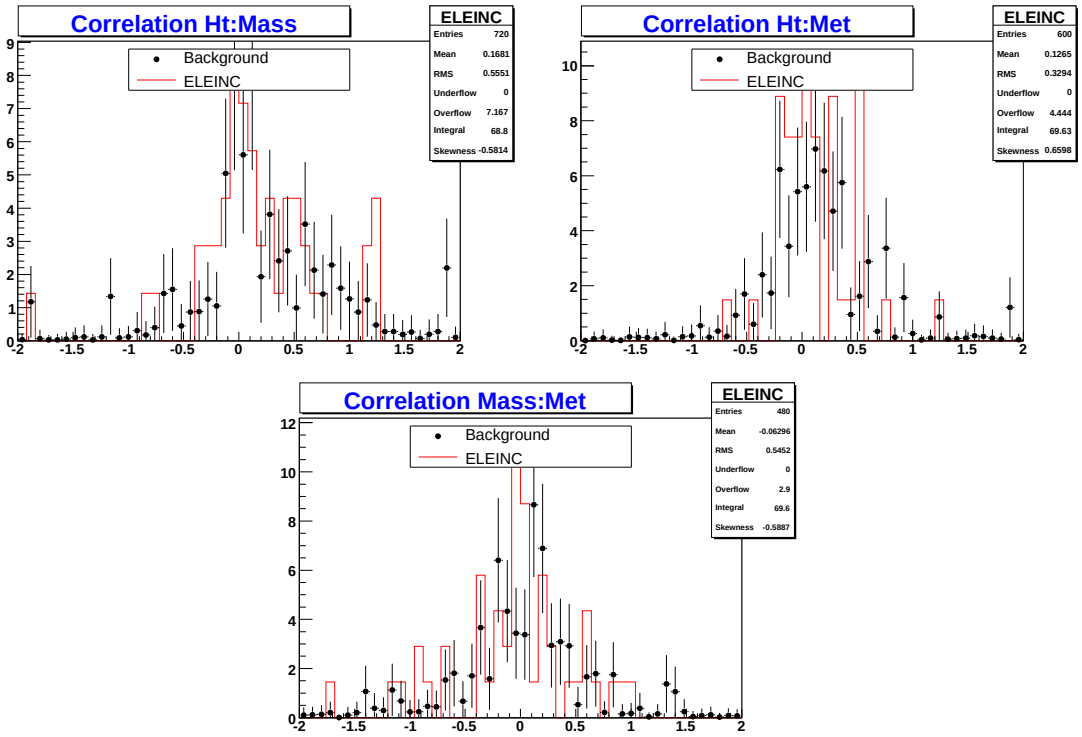

Figure 6: Distribution of the correlation coefficients in single tight tagged electron data compared to the appropriate mix of backgorund events. Histograms are normalized to equal area.

6.3 Test of Neural Network output

The most critical check of the validity of the Neural Net is, however, the comparison of the Neural Net distribution itself for the pretag sample. The 1-dimensional projections onto the x and y-axes are shown in Fig. 7. The x-axis is used to discriminate between Z+jets and ZH, the y-axis is used to discriminate between $t\bar{t}$ and ZH. We again plot simuletaneously the Alpgen+Herwig and Pythia simulations.

We also compare the data and MC after making further cuts on the NN variables. The signal is expected to be at $(0, 1)$, the $t\bar{t}$ background at $(1, 1)$ and the other backgrounds mostly at $(0, 0)$. To test the Z+jets background we now select events with $y_{NN} < 0.25$ to suppress the $t\bar{t}$ background, and for testing the $t\bar{t}$ we select events with $x_{NN} > 0.75$ to suppress the Z+jets background. These plots are shown in Fig. 8 for electrons and muons, combined.

In general, the Alpgen+Herwig sample is in good agreement with the data. However, because discrepencies exist, the Pythia sample will be used as a systematic error on our background shapes.

6.4 Comparisons of Data and Simulation in the b-tagged Sample

Finally we compare the data and the simulation in the b-tagged sample. Here we currently require at least two loose b-tagged jets in one channal. If we do not find the two loose tags in an event we search for at at least one tight b-tagged jet. The comparisons are made using Alpgen for the $Z + 2b$ background, i.e. our default model for the background. We compare electrons and muons separately. For this comparison the AlpGen MC is normalised to the NLO cross section. We are still in the processs of cross-checking this normalisation.

Fig. 9 and 10 show comparisons of data and MC for many kinematic properties of the events of the single tagged events, Fig. 11 and 12 for the double tagged. The data agree well with the Standard Model backgrounds within the current statistical uncertainties.

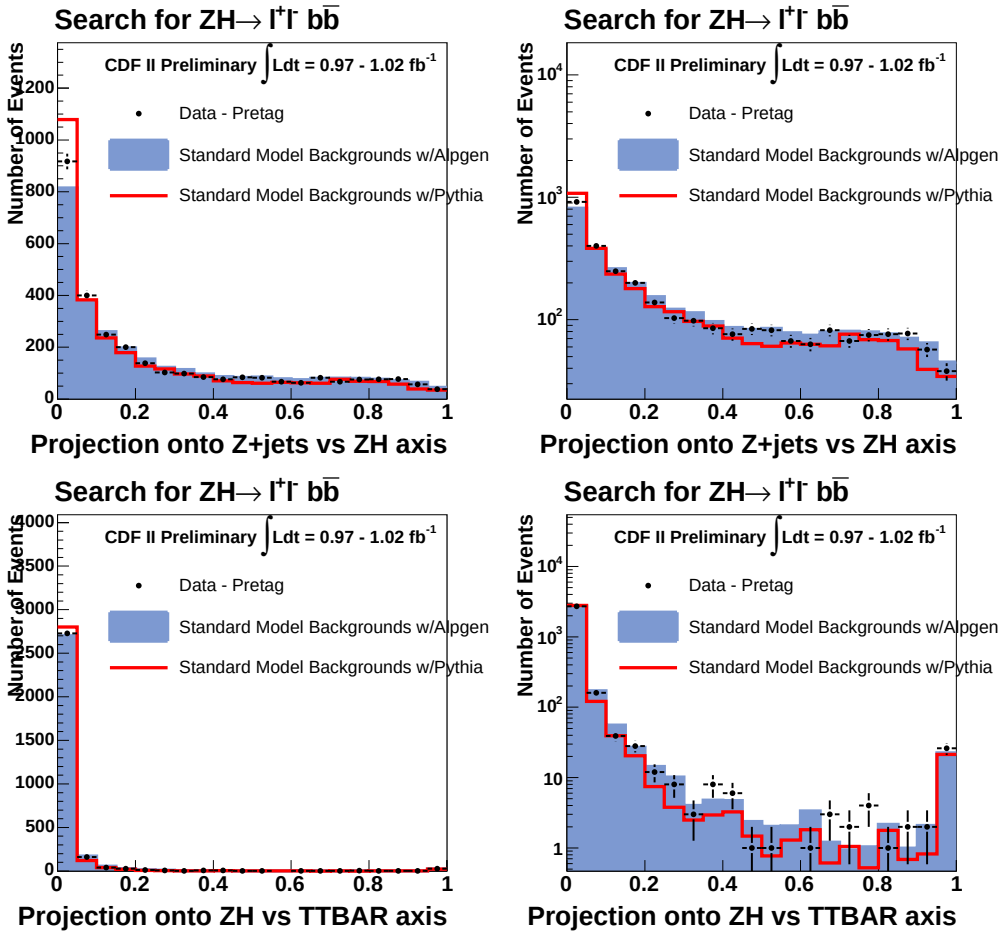

Figure 7: Pretagged data compared to Monte Carlo expectation shown are the projections of the NN onto the x-axis (upper plots in linear and logarithmic scale) and y-axis (lower plots) The MC which usesthe Alpgen+Herwig montecarlo simulations are in blue, pythia is represented with the red line.

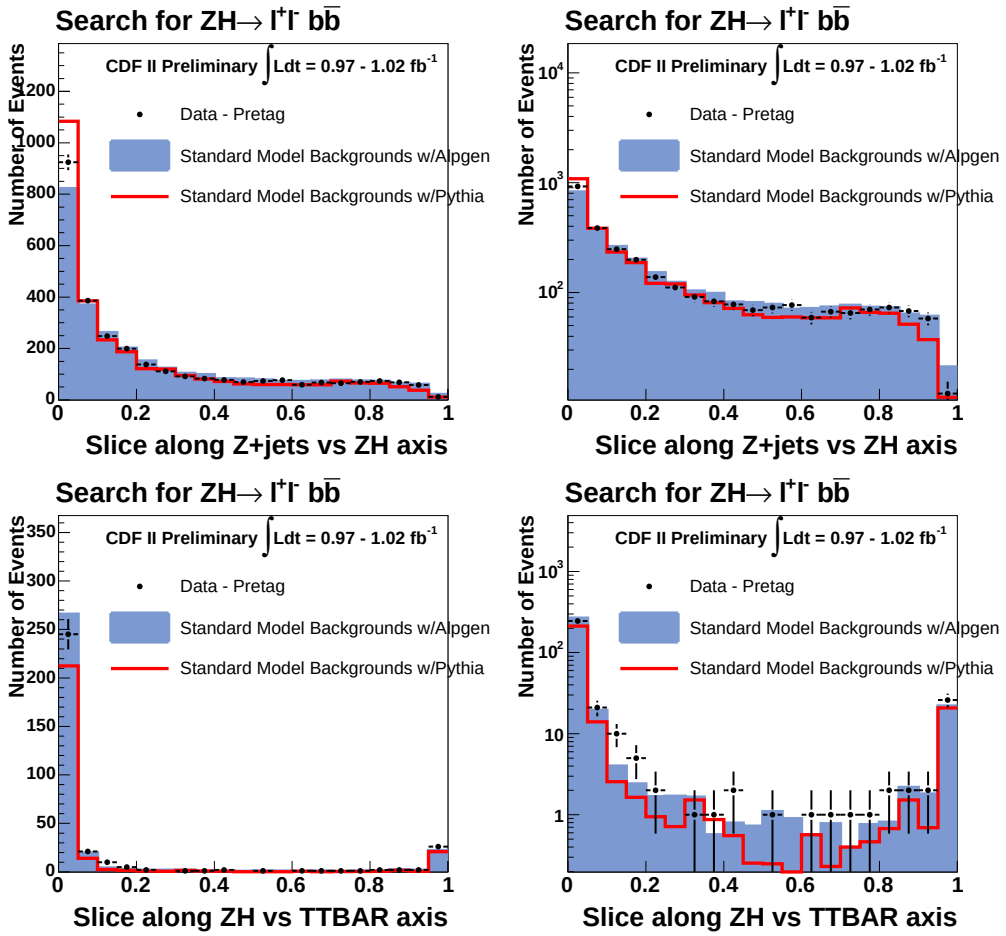

Figure 8: Pretagged data compared to Monte Carlo expectation shown are the projections of the NN onto the x-axis (upper plots in linear and logarithmic scale) and y-axis (lower plots) The MC which usesthe Alpgen+Herwig montecarlo simulations are in blue, pythia is represented with the red line. After selecting events with $x_{NN} > 0.75$ (top plots) and $y_{NN} < 0.25$ (bottom plots).

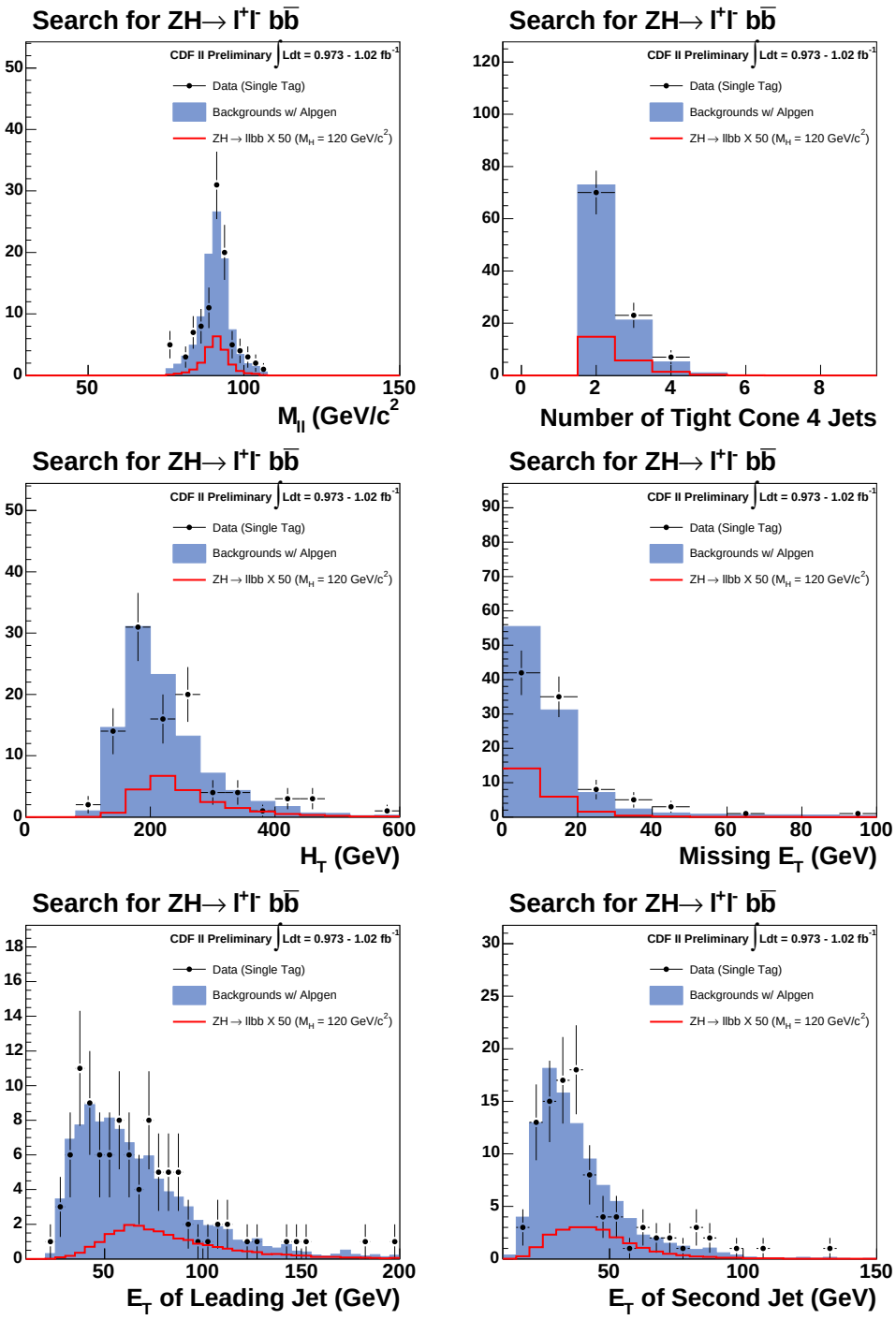

Figure 9: Single tagged data compared to Monte Carlo expectation. The MC which uses the Alpgen+Herwig montecarlo simulations are in blue, ZH ($M_H = 120$ GeV/c^2) is represented with the red line and scaled to 100 times expected value: invariant dilepton mass (upper left), number of jets (upper right), H_T (middle left), missing E_T (middle right), E_T of leading (lower left) and subleading (lower right) Jets.

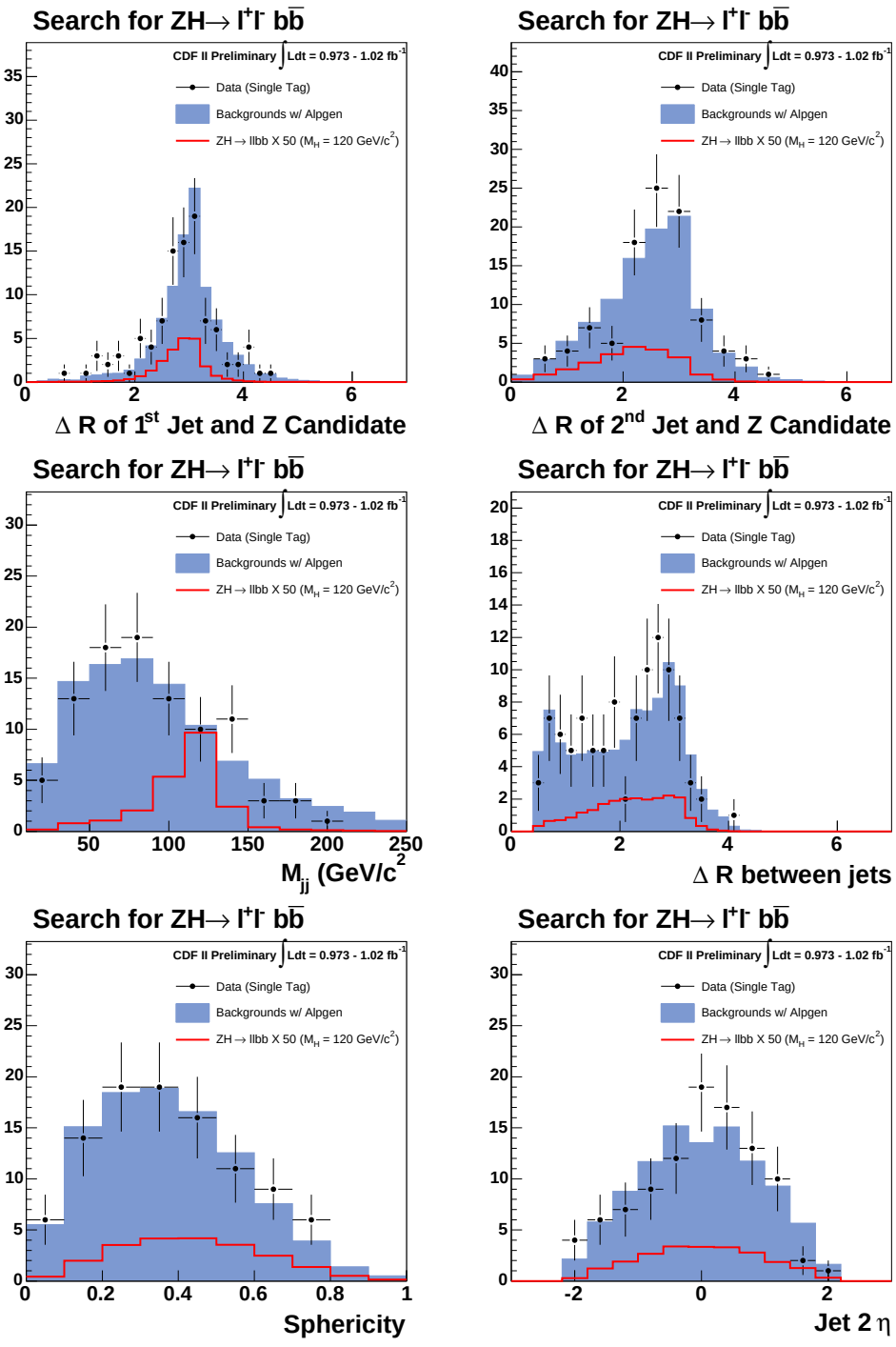

Figure 10: Single tagged data compared to Monte Carlo expectation. The MC which uses the Alpgen+Herwig montecarlo simulations are in blue, pythia is represented with the red line: ΔR of leading jet and Z (upper left), ΔR of second jet and Z (upper right), invariant mass of two leading jets (middle left), ΔR of leading and second jets (middle right), sphericity of 4 relevant objects (bottom left), η of second jet (bottom right.)

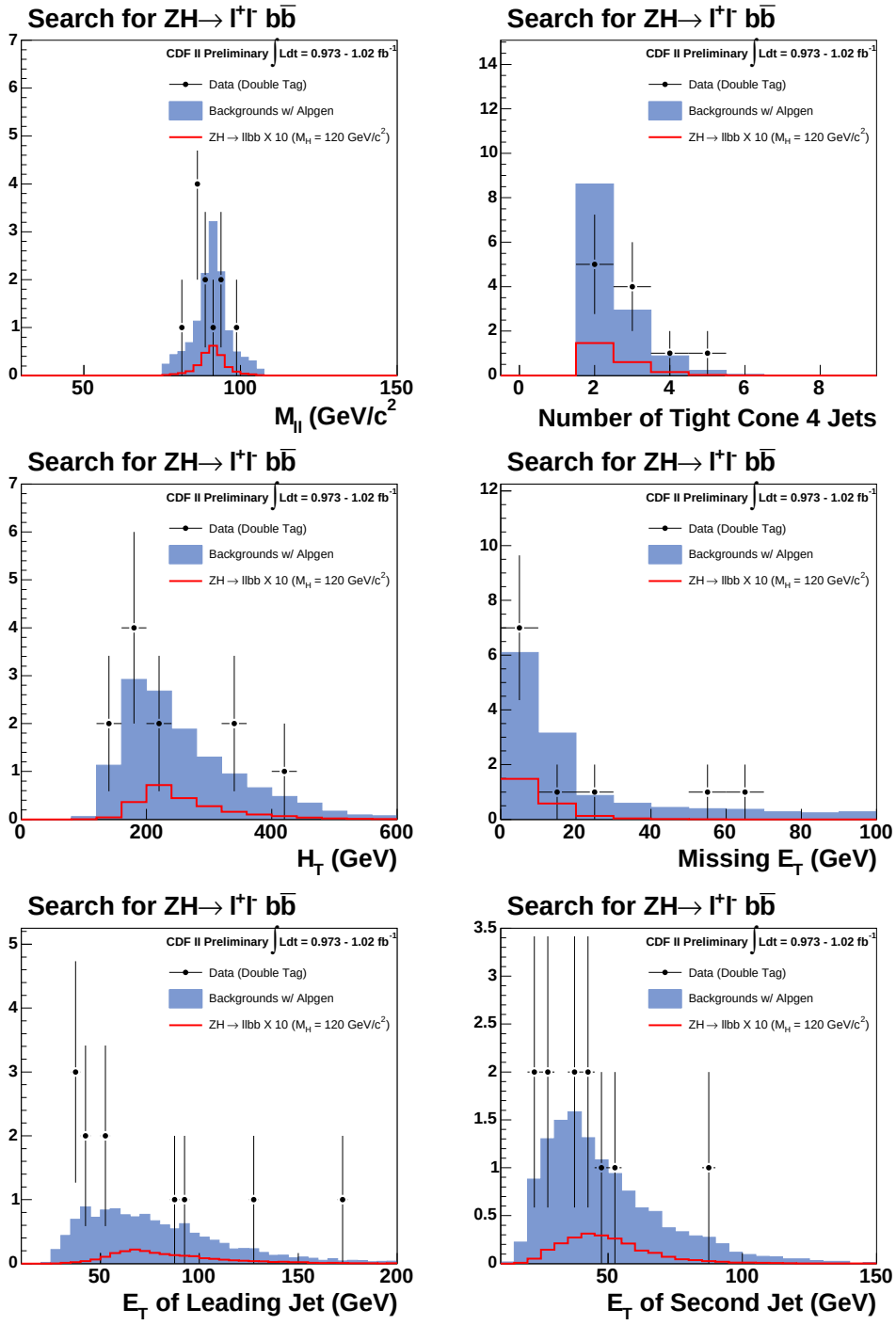

Figure 11: Double tagged data compared to Monte Carlo expectation. The MC which uses the Alpgen+Herwig montecarlo simulations are in blue, ZH ($M_H = 120$ GeV/c^2) is represented with the red line and scaled to 50 times expected value: invariant dilepton mass (upper left), number of jets (upper right), H_T (middle left), missing E_T (middle right), E_T of leading (lower left) and subleading (lower right) Jets.

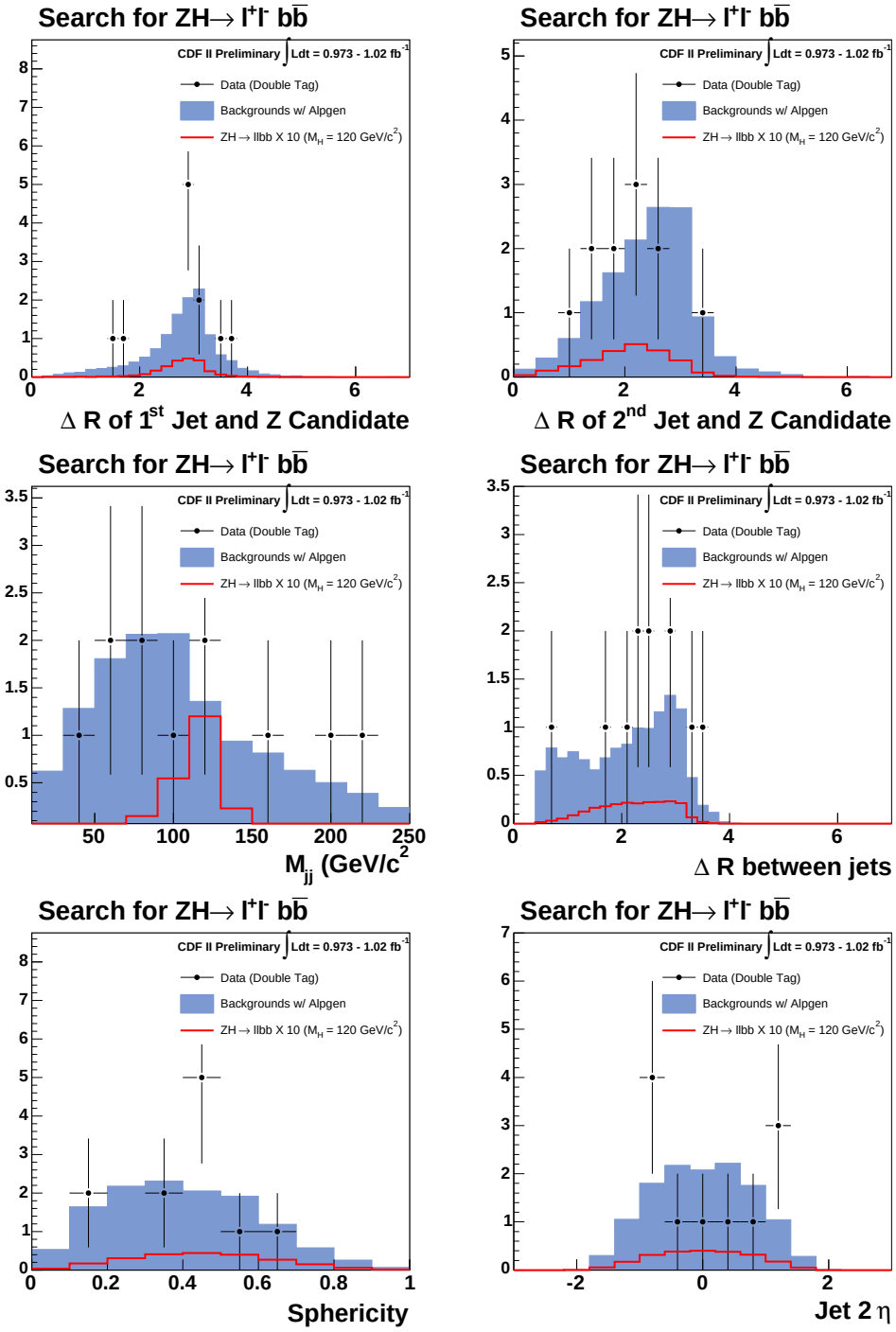

Figure 12: Double tagged data compared to Monte Carlo expectation. The MC which uses the Alpgen+Herwig montecarlo simulations are in blue. ZH (M_H = 120 GeV/c^2) is represented with the red line and scaled to 50 times expected value: ΔR of leading jet and Z (upper left), ΔR of second jet and Z (upper right), invariant mass of two leading jets (middle left), ΔR of leading and second jets (middle right), sphericity of 4 relevant objects (bottom left), η of second jet (bottom right.)

7 Systematic Uncertainties

We consider the following sources of systematic uncertainties on the normalisation of the backgroudn sources:

- an uncertainty of 40% on the normalisation of the $Z+b\bar{b}$ and $Z+c\bar{c}$ backgrounds due to the uncertainty on the NLO cross section. This is consistent also with the uncertainty on the W+heavy flavour backgrounds in the WH analysis.
- an uncertainty of 20% on the $t\bar{t}$, WZ and ZZ normalisation. This uncertainty includes the cross section uncertainty.
- an 8% uncertainty on the normalisation of the mistag background due to the mistag matrix and an uncertainty of ± 0.15 on the mistag asymmetry factor of 1.37. An additional factor on the mistag matrix of 1.05 ± 0.03 and 1.07 ± 0.05 is taken for the 0h and 0i data respectively. The total uncertainty on the mistag prediction is 13%.
- an 8% uncertainty on the SecVtx tagging efficiency for b-jets and a 16% uncertainty on the SecVtx tagging efficiency for c-jets. This affects the ZH signal, and the $Z+b\bar{b}$, $Z+c\bar{c}$, $t\bar{t}$, WZ and ZZ backgrounds.
- a 1% uncertainty on the trigger efficiencies and lepton identification efficiencies. This is correlated between the ZH signal, and the $Z+b\bar{b}$, $Z+c\bar{c}$, $t\bar{t}$, WZ and ZZ backgrounds.
- a 50% uncertainty on the fake Z background.
- a 6% uncertainty on the integrated luminosity. This affects all the MC samples.

In addition we consider the following uncertainties that change the shape of the NN distribution:

- the jet energy scale is applied to both signal and background samples to study the influence. It is treated to be correlated among all MC samples of signal and background.
- the difference between using Alpgen and Pythia for the Z+ heavy flavour backgrounds is taken as a systematic uncertainty. In the most signal like regions this is about a 30% effect.

- for signal we consider systematic uncertainties due to initial and final state QCD radiation and due to the parton distribution functions. We use the prescription from the Joint Physics webpages for both these effects.

- for $t\bar{t}$ production we estimate a systematic uncertainty using Herwig, and comparing that to Pythia. The contribution in the signal area of the NN distribution is very small though. So, it has a negligible effect.

The systematic uncertainties on the shapes are shown in Figure 13 for the x-axis projection of the NN output variable.

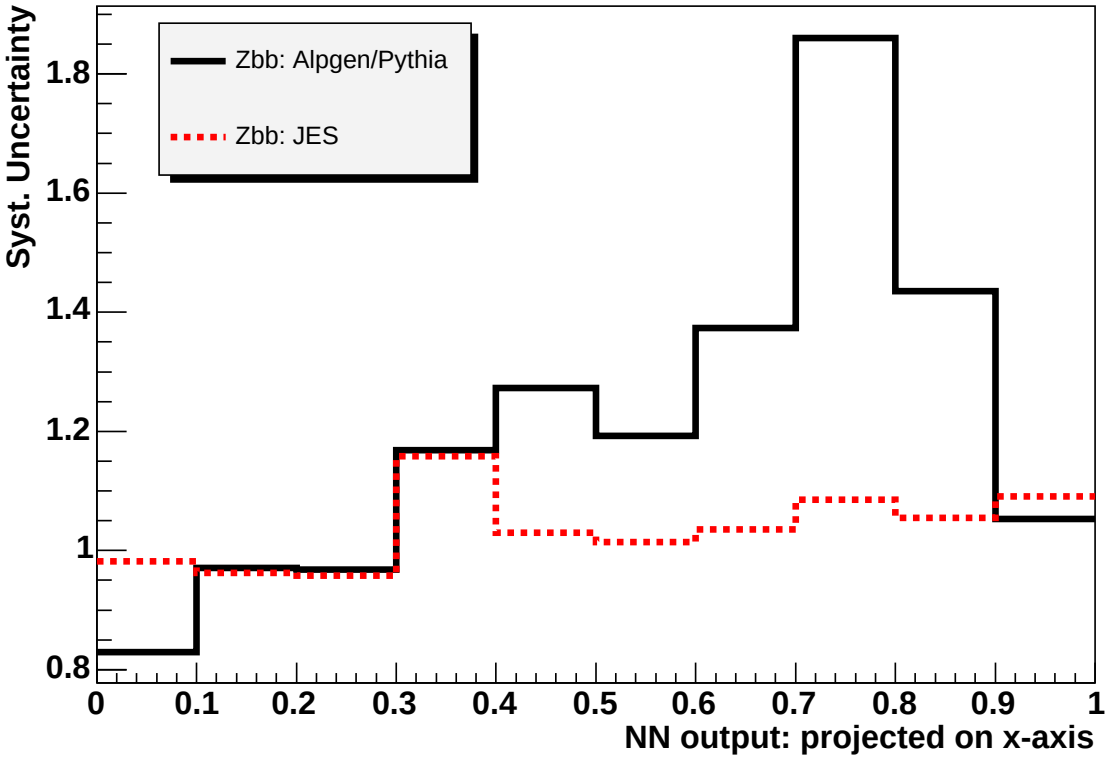

Figure 13: The shape systematic uncertainties for the $Z + h.f.$ background (left) and the ZH signal (right). Shown is the effect on the NN projection along the x-axis for $y_{NN} < 0.5$.

We evaluate systematic uncertainties by doing pseudoexperiments where we assume our default likelihood function, and evaluate how our expected 95% CL upper limit changes when we input a different model of signal or background. For shape systematics, we choose

events for our pseudoexperiments from systematically altered templates, and also take into consideration changes in expected event yields due to the effect of the systematic. The different shapes are inputs into our limit setting procedure outlined below.

Our major systematic is the difference of modeling the $Z+jets$ background using Alpgen verses Pythia. While Alpgen is in good agreement with the data for jet multiplicity, it tends to overestimate the E_T of the jets and several other energy related distributions. Pythia, on the other hand, underestimates the energy of these distributions. Since Alpgen does a better job of modeling the NN Output distribution, but the data falls between Pythia and Alpgen for the input kinematics, we assign a shape systematic due to the difference in modeling of the $Z + jets$ background.

Other shape systematics include the jet energy scale which we determine by fluctuating the jet energy scale in all processes by 1 sigma, and the ISR and FSR systematics which we determine by comparing nominal signal MC using the "more or less" prescription of Pythia generation parameters outlined by Un-Ki Yang. We also include shape systematics for the mistag shape. Since the weighting of pre-tagged events grows as a function of their E_T, uncertainties in the mistag matrix could affect the signal region differently than the background region. We determine new mistag shapes by fluctuating the mistag matrix weights applied to jets systematically up or down by their uncertainty. Finally, we evaluate a further shape systematic due to the mismodeling of the $\not\!\!E_{\rm T}$ distribution. Electroweak Z Pythia with minimum bias events overlayed does a better job of predicting the $\not\!\!E_{\rm T}$ distribution, but we do not have such MC for the $Z+$ heavy flavor process, and so we model $Z + jets$ with top MC not having extra interactions. We evaluate the systematic of this assumption using pseudoexperiments modeled with the electroweak $Z + l.f.$ Pythia.

The table of systematics are listed in Table 14.

8 Results

After verifying that the data are well modeled in both the pretag and the tagged sample the Neural Net is applied to the data. The resulting NN output distribution for the data is shown in Fig. 14. We observe the expected three contributions, the peak at $(1, 1)$ is mostly

Systematic uncertainties and shift of σ in pb	
Background Shape (Pythia vs Alpgen)	0.17
Jet energy scale	0.08
ISR gluon radiation	0.02
FSR gluon radiation	0.04
PDF reweighting	0.00
Total systematic	0.19

Table 14: Summary of uncertainties in terms of shift of expected 95% CL upper limit exclusion limit.

due to $t\bar{t}$, the events at $(0,0)$ mostly due to Z+jets and the signal is expected near $(1,0)$.

The 1-dimensional projections along the x- and y-axes are shown in Fig. 15 and 16 for single tagged and double tagged, respectively. The data agree well with the background predictions. In particular at the low and high values of the NN output the data confirm the $t\bar{t}$ and $Z+$ jets background estimates.

Also shown in these figures are the NN projections after applying a cut on the other axes, i.e. for the x-axis projection a cut on $y_{NN} < 0.25$ is applied and for the y-axis projection a cut on $x_{NN} > 0.75$ is applied to clearly show how the data compare in the region most sensitive to ZH production. Again good agreement is observed between data and the Standard Model prediction.

Our 95% cross-section limit on σ_{ZH} is done using the mclimit technique described in CDF note 8124, Ref.[9]. This technique handles all our shape and normalization systematics. The final expected and observed limits are shown in Table 15 as ratios compared to the Standard Model expected values. These are better than the limits from the summer 2006.

In our double tagged channal, we have found one event event in the corner of the Higgs Region. It is dimuon event with a Z mass of 97 GeV/c^2. The dijet mass of the object is 119.8 GeV/c^2. It has a SANN value of 0.96 in the ZH vs. Z+jets access and .005 in the ZH vs $t\bar{t}$ axis. Displays of the event can be seen in Figure [**?**]. We have calculated that the signal to Background of this bin of our selection artificial neural network is 1/4.2.

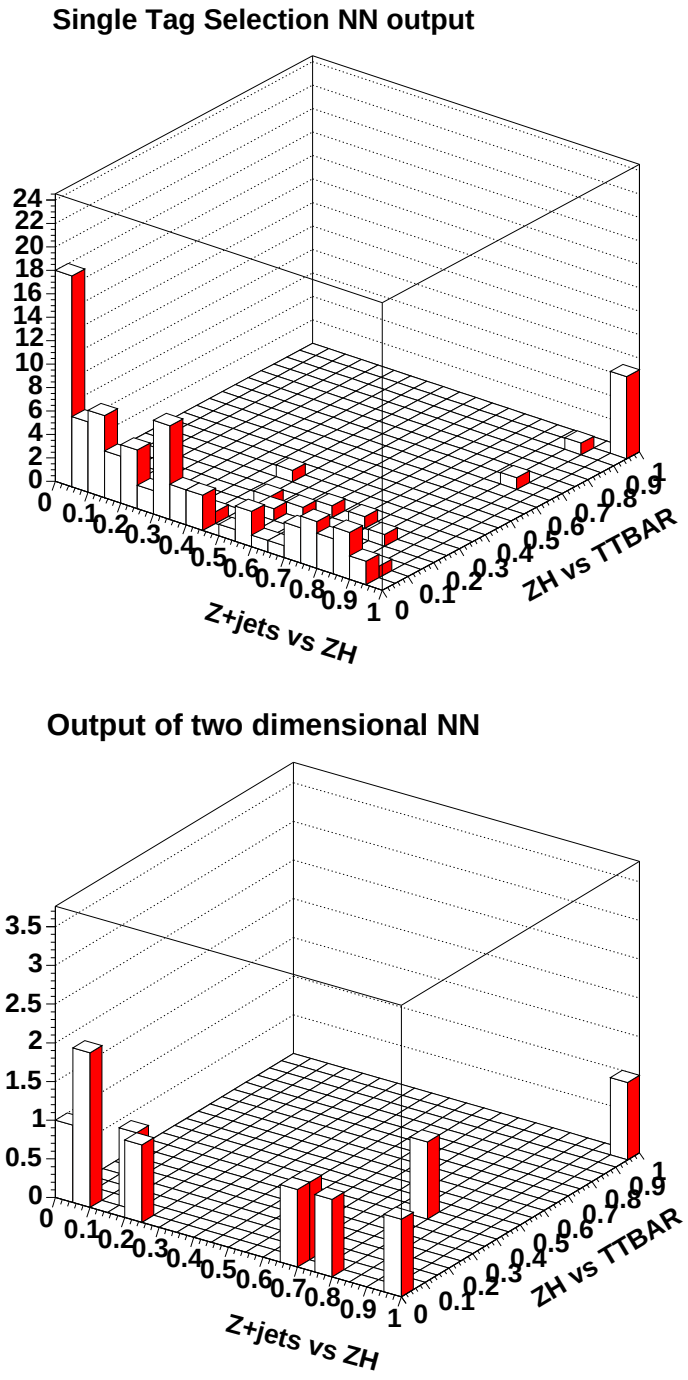

Figure 14: The NN output distribution for the electron and muon data combined. Above single tags, below double tags. The $t\bar{t}$ background is expected in the upper right corner, the $Z+$ jets in the lower left and the ZH signal in the lower right.

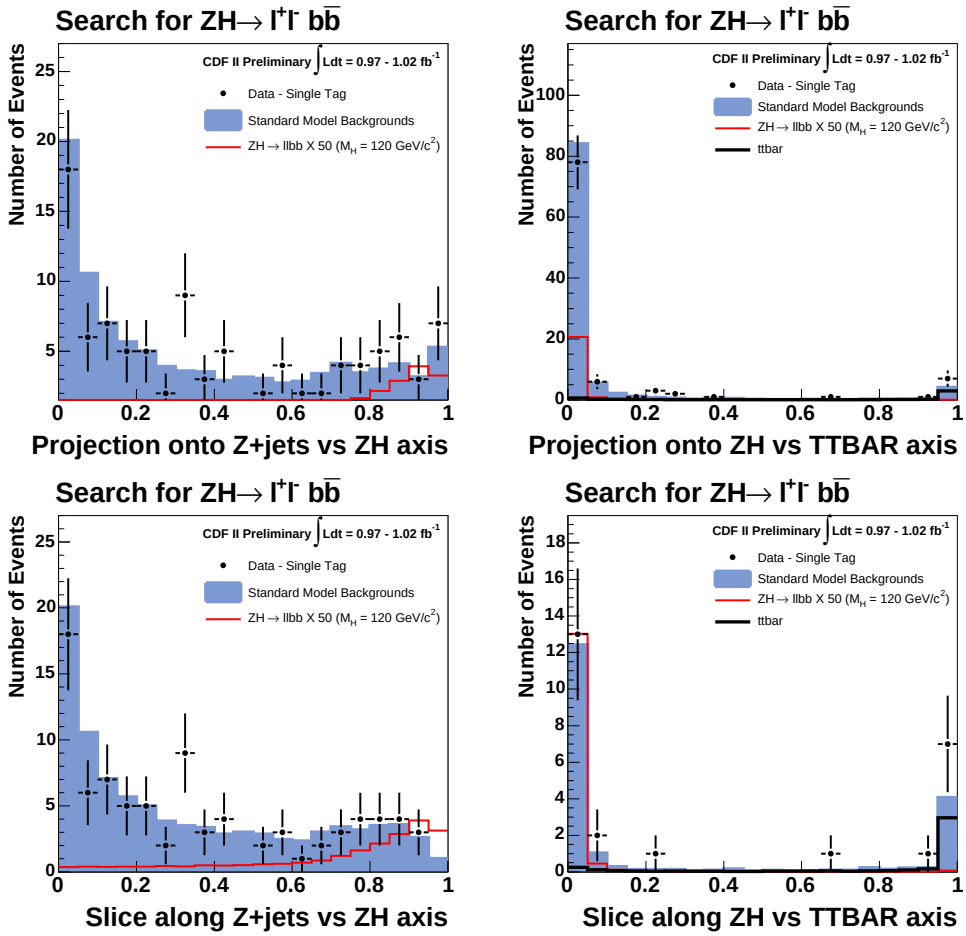

Figure 15: Single tagged data compared to Monte Carlo expectation shown are the projections of the NN onto the x-axis (upper left) and y-axis (Upper right). Projections of the slice are displayed along the x-axis (bottom left) and y-axis (lower right). The cuts in these plots are $y \leq .25$ and $x \geq .75$, respectively. The MC which usesthe Alpgen+Herwig montecarlo simulations are in blue, ZH (M_H=120 GeV/c^2) is represented with the red line.

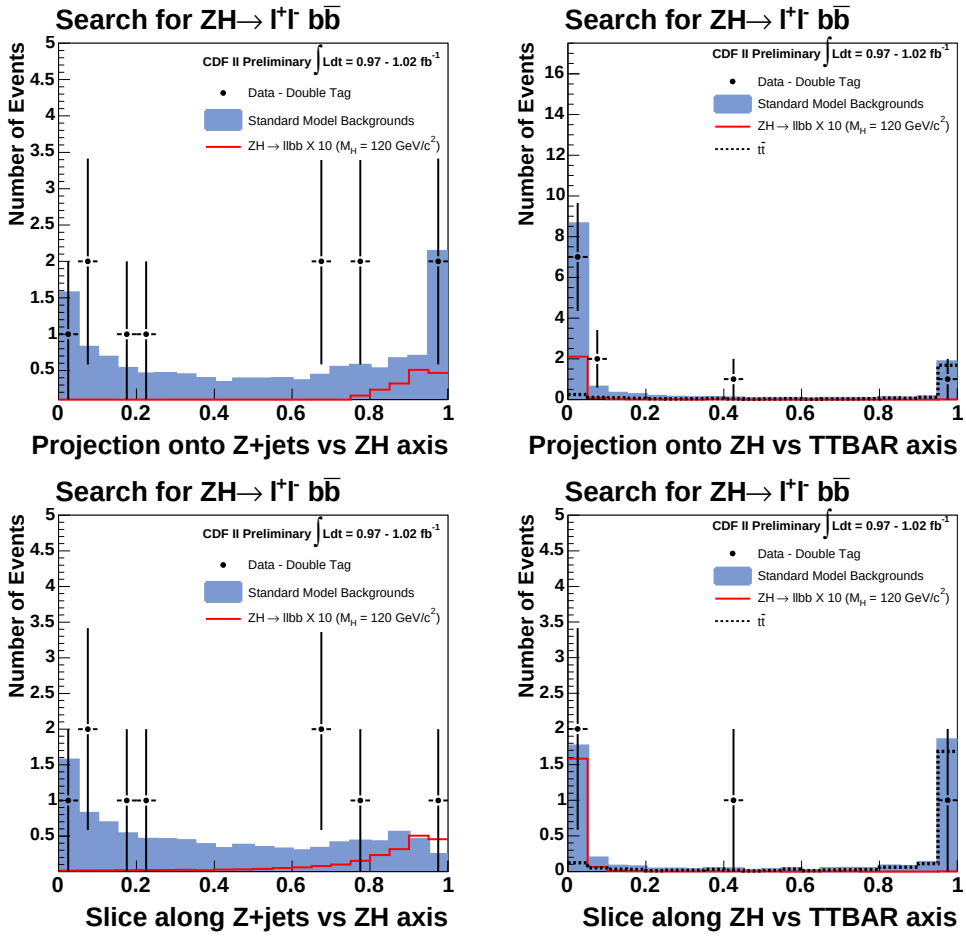

Figure 16: Double tagged data compared to Monte Carlo expectation shown are the projections of the NN onto the x-axis (upper plots in linear and logarithmic scale) and y-axis (lower plots). Projections of the slice are displayed along the x-axis (bottom left) and y-axis (lower right). The cuts in these plots are $y \leq .1$ and $x \geq .9$, respectively. The MC which usesthe Alpgen+Herwig montecarlo simulations are in blue,ZH (M_H=120 GeV/c^2) is represented with the red line.

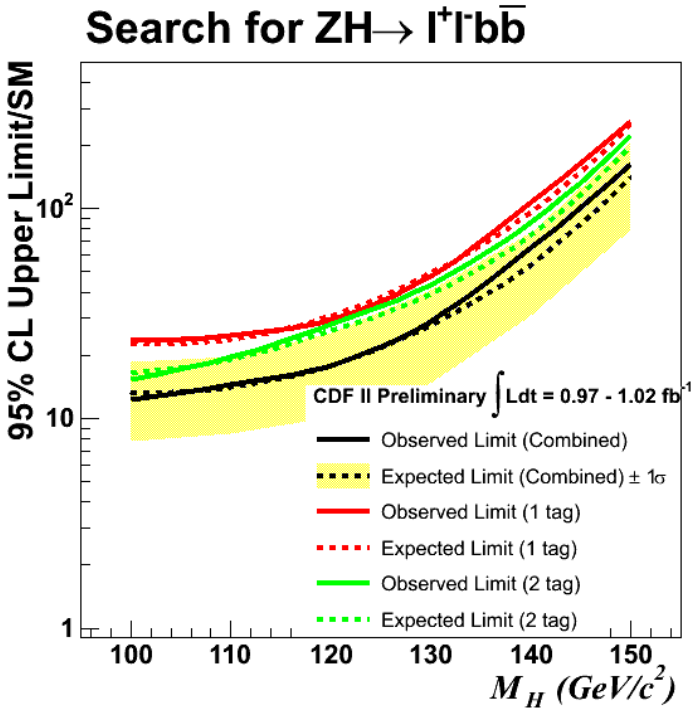

Figure 17: Expected and observed limits from the data as a ratio compared to expected Standard Model cross-sections (95% CL XSec / SM). Single-tag and double-tag samples are shown separate and combined.

Mass (GeV/c^2)	1-tag Obs. Limit (Exp.)	2-tag Obs. Limit (Exp.)	Comb. Obs.Limit(Exp.)
100	23.4 (22.8)	15.4 (16.5)	12.4 (13.2)
110	24.8 (23.8)	19.6 (19.2)	14.4 (14.1)
115	27.5 (27.3)	23.1 (22.5)	16.3 (16.2)
120	Old (Summer 2006 1 fb^{-1} single taggged only)		30.7 (26.2)
120	29.6 (30.7)	28.0 (26.1)	17.9 (17.8)
130	47.7 (49.3)	43.4 (39.3)	29.1 (27.8)
140	107 (96.1)	85.7 (74.7)	65.1 (54.2)
150	260 (252)	225 (200)	163 (142)

Table 15: Expected and observed limits from the data as a ratio compared to expected Standard Model cross-sections (95% CL XSec / SM). Single-tag and double-tag samples are shown separate and combined. The result obtained during the previous iteration of this analysis, over the same data set, is included for comparison. It was obtained by looking only in single tagged events.

9 Conclusions and Future Directions

We are considering several avenues to improve our sensitivity including increasing acceptance, additional triggers, improving jet resolutions, and using additional b-tags.

References

[1] J. Efron, B. Kilminster, B. Heinemann, A. Mehta, R. Hughes, B. Parks, B. Winer, *Search for ZH in 1 fb*$^{-}$1, CDF note 8363

[2] http://www-cdf.fnal.gov/internal/dqm/goodrun/good.html

[3] B. Heinemann, *Summary of Most Commonly used Scale Factors for the 2006 Summer Conferences*, CDF note 8312 (and references therein)

[4] M. Griffiths, B. Heinemann, G. Manca, *Fake Rate For Low-p_T Leptons*, CDF note 7470

[5] A. Mehta, B. Heinemann, *Measurement of the b jet cross section for events with a Z^0 boson*, CDF note 7780

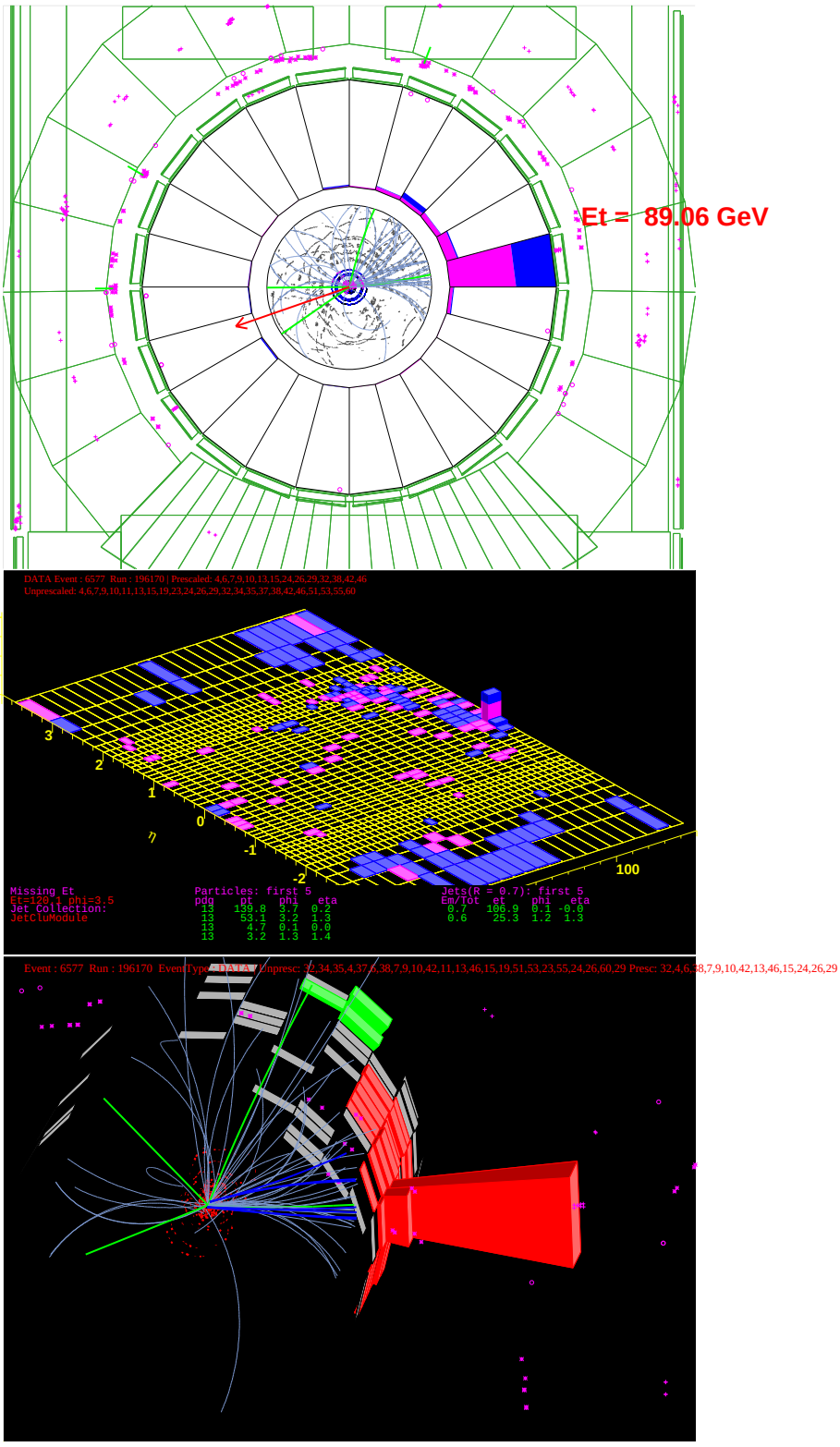

Figure 18: Various event displays of event in our Higgs corner in the double tagged regiou. It is a dimuon event with a Z mass of 97.3 GeV/c^2 and a dijet mass of 119.8 GeV/c^2.

[6] S. Budd, T. Junk, T. Liss, andC. Neu, *Tight, Loose and Ultratight SECVTX Tag Rate Matrix with 1.2 fb^{-1}*, CDF note 8519

[7] Grinstein, Guimararaes da Costa, and Sherman, *SecVtx Mistag Asymmetry for Winter 2007*, CDF note 8626

[8] B. Parks, R. Hughes, B. Kilminster, K. Lannon, B. Winer, *Multi-jet Energy corrections using a Neural Net*, CDF 8124

[9] T. Junk, *Sensitivity, Exclusion and Discovery with Small Signals, Large Backgrounds, and Large Systematics*, CDF note 8128

[10] C. Neu *"How to Determine the Number of Mistagged Jets"'* http://ww-cdf.fnal.gov/internal/physics/top/RunIIBtag/mistags.ps